DTU Library

Size-dependent escape risk of lumpfish (Cyclopterus lumpus) from salmonid farm nets

Herrmann, Bent; Sistiaga, Manu; Jørgensen, Terje

Published in:
Marine Pollution Bulletin

Link to article, DOI:
10.1016/j.marpolbul.2020.111904

Publication date:
2021

Document Version
Peer reviewed version

Citation (APA):
Herrmann, B., Sistiaga, M., & Jørgensen, T. (2021). Size-dependent escape risk of lumpfish (*Cyclopterus lumpus*) from salmonid farm nets. *Marine Pollution Bulletin*, *162*, Article 111904. https://doi.org/10.1016/j.marpolbul.2020.111904

Marine Pollution Bulletin

Size-dependent escape risk of lumpfish (Cyclopterus lumpus) from salmonid farm nets

--Manuscript Draft--

Manuscript Number:	MPB-D-20-01815R1
Article Type:	Research Paper
Keywords:	Lumpfish; fish farming; escape risk; fish morphology; FISHSELECT
Corresponding Author:	Bent Herrmann, Ph.D SINTEF Ocean Hirtshals, DENMARK
First Author:	Bent Herrmann, Ph.D
Order of Authors:	Bent Herrmann, Ph.D
	Manu Sistiaga, Ph.D
	Terje Jørgensen, Ph.D
Abstract:	In the last decade, the salmon aquaculture industry has considerably increased the use of lumpfish juveniles as cleaner fish. Potential escape of reared lumpfish into the wild may spread diseases or genetically contaminate wild stocks. The guidelines for minimum sizes of cleaner fish to use in aquaculture cages are currently based on simple mesh penetration tests. However, these guidelines do not consider the potential compressibility of fish or changes in mesh state due to factors such as sea conditions and maintenance operations. This study shows that the industry-recommended minimum stocking sizes for a given mesh size may result in escape risk and that ignoring fish compressibility and mesh state can lead to underestimation of the lumpfish sizes that are able to escape. Our results can be used to develop new guidelines that will contribute to reduced escape of lumpfish from salmonid farms and lessen the potential environmental consequences.

Size-dependent escape risk of lumpfish (*Cyclopterus lumpus*) from salmonid farm nets

Bent Herrmann[1,2,3e*], Manu Sistiaga[4,5e], Terje Jørgensen[4e]

[1] SINTEF Ocean, Brattørkaia 17C, N-7010 Trondheim, Norway

[2] The Arctic University of Norway, UiT, Breivika, N-9037 Tromsø, Norway

[3] DTU Aqua, Technical University of Denmark, Hirtshals, Denmark.

[4] Institute of Marine Research, Postbox 1870 Nordnes, N-5817 Bergen, Norway

[5] Norwegian University of Science and technology, Otto Nielsens veg 10, N-7491 Trondheim, Norway

e: equal authorship

* Corresponding author. Tf: +4529617964

E-mail address: bent.herrmann@sintef.no

Abstract

In the last decade, the salmon aquaculture industry has considerably increased the use of lumpfish juveniles as cleaner fish. Potential escape of reared lumpfish into the wild may spread diseases or genetically contaminate wild stocks. The guidelines for minimum sizes of cleaner fish to use in aquaculture cages are currently based on simple mesh penetration tests. However, these guidelines do not consider the potential compressibility of fish or changes in mesh state due to factors such as sea conditions and maintenance operations. This study shows that the industry-recommended minimum stocking sizes for a given mesh size may result in escape risk and that ignoring fish compressibility and mesh state can lead to underestimation of the lumpfish sizes that are able to escape. Our results can be used to

develop new guidelines that will contribute to reduced escape of lumpfish from salmonid farms and lessen the potential environmental consequences.

Keywords: Lumpfish; fish farming; escape risk; fish morphology; FISHSELECT

1. Introduction

The boom of the salmon (*Salmo salar*) aquaculture industry in the last 20 years has led to high densities of fish in sea cages, and this crowding has resulted in challenges with parasitism and disease outbreaks that compromise the sustainability and welfare of the industry (Aaen et al., 2015). The salmon louse (*Lepeophtheirus salmonis*) is a common parasite on wild salmonids, but in high numbers it can cause significant external damage that can lead to serious infections and death (Wootten et al., 1982). It has a huge negative economic impact on salmon farming companies, and in Norway the industry spends millions of dollars every year to remove this parasite from the fish (Torrissen et al., 2013; Abolofia et al., 2017). For years, parasitized salmon have been treated with chemical baths or mechanical treatments (Overton et al., 2019), but these methods can harm the environment and the fish. Therefore, the use of cleaner fish has become increasingly popular (Gonzalez and de Boer, 2017; Brooker et al., 2018; Foss et al., 2020).

Today, the salmon farmers in Norway use two families of cleaner fish to remove parasites: wrasses (e.g., Ballan wrasse (*Labrus bergylta*) and goldsinny wrasse (*Ctenolabrus rupestris*)) and lumpfish (*Cyclopterus lumpus*). Wrasses have been used for many years (Bjørdal, 1991), whereas the use of lumpfish is more recent (Imsland et al., 2014a,b). The use of lumpfish is gaining popularity among farmers because unlike wrasses, which stop feeding at temperatures below 6°C (Sayer and Reader, 1996), they perform well at low water temperatures and can be used for delousing purposes year-round (Imsland et al., 2016). The industry in Norway uses approximately 30 million juvenile lumpfish each year for delousing purposes (Foss et al., 2020). Juvenile lumpfish are more effective at delousing and have less impact on salmon growth than larger lumpfish individuals (Imsland et al., 2014c; Foss et al., 2020).

Juvenile lumpfish are produced by the salmon aquaculture industry. However, the production of these juveniles requires harvesting wild mature individuals for use as broodstock (Powell, et al., 2018a). Until recently, this species was only harvested for its roe (Johanesson 2006; Kennedy et al., 2019), but the demand from the aquaculture industry for mature adult individuals has increased fishing pressure (Powell et al., 2018a) on a species that already is classified as near threatened on the IUCN Red List (Lorance et al., 2015). The increased use of juvenile lumpfish in salmonid farms has raised various environmental and welfare issues as well (Geitung et al., 2020), including potential impact on wild stocks of lumpfish and high mortality rates of them (Imsland et al., 2020; Klakegg et al., 2020). The potential escape of lumpfish from sea cages also is concerning. In a recent review, Powell et al. (2018a) highlighted the need to critically assess the risk of farmed lumpfish escaping from net pens because escapees can interbreed with local populations and result in genetic introgression, as was previously observed for salmonids escaping from farms (Consuegra et al., 2011). There are five genetically distinct lumpfish groups located in the West Atlantic (USA and Canada), Mid Atlantic (Iceland), East Atlantic (Faroe Islands, Ireland, Scotland, Norway and Denmark), English Channel (England) and Baltic Sea (Sweden) and the genetic diversity within these groups is low, meaning that genetic introgression represents a particularly important threat for this species (Whittaker et al., 2018). According to Jonassen et al. (2018) and Treasurer et al. (2018), eggs and lumpfish juveniles are translocated across the north Atlantic and upon escape these fish can pose a threat to local populations. Treasurer et al. (2018) and Bolton-Warberg et al. (2018) reported respectively that approximately 85 % of the lumpfish used in Scotland in 2017 and 70% of the individuals used in Ireland in the period 2015-2016, were of Icelandic and Norwegian origin and none of them from local origin, meaning that parental source locations likely are mixed.

Small lumpfishes are more effective at delousing salmon than larger individuals, which increases the motivation for farmers to employ smaller individuals in the farms (Imsland et al. 2014a,b,c). Imsland et al. (2016) reported that lumpfish with total length between 10 and 18 cm (~50–180 g) have good delousing traits, but in Norway the most commonly used sizes are fish between 6 and 9 cm long (~20 and 30 g) (Salmar AS, Personal communication). However, the use of small lumpfish increases the risk of escape through cage nettings. Salmon farmers traditionally used square meshes of 30–50 mm (Moe et al., 2007), but the mesh sizes used in salmon cages can vary greatly. User guidelines are based on mesh penetration tests, but these tests do not properly account for variability in the condition and compressibility of fish of different sizes (Harboe and Skulstad, 2013). Moreover, earlier studies showed that in addition to mesh size, alterations in mesh state can increase the escape risk of fish through netting meshes (Herrmann et al., 2016a; Sistiaga et al., 2020). Square meshes can adopt different shapes and tension states (bars under tension or slack) due to netting manipulation during maintenance operations and variation in sea conditions (e.g., currents, waves) (Huang et al., 2006; Lader et al., 2008; Sistiaga et al., 2020). The latter represents an increased risk for cages placed in more exposed sea areas, which is a growing trend in the industry due to increased demand for farming sites (Jónsdóttir et al., 2019).

Despite the importance of lumpfish as cleaner fish, no scientific study has been conducted to investigate which sizes of this species can be used safely in salmon cages without risking escape. Therefore, the aim of this study was to evaluate the potential effect of mesh size and mesh state on the escape risk of lumpfish and predict the minimum size of lumpfish that can be safely used in aquaculture cages.

2. Materials and Methods

2.1. Effect of mesh shape and state vs. lumpfish size and morphology on potential escape through cage netting

For a lumpfish to pass through cage netting two conditions must be fulfilled. First, the fish needs to contact the netting at an orientation that gives it a size-dependent possibility of passing through the mesh of the netting (Sistiaga et al., 2010). Second, the fish needs to be morphologically able to pass through the mesh. Therefore, the main factors to consider in the escape risk of lumpfish from fish farming cages are size, shape, and state of the mesh in relation to size, morphology, and tissue compressibility of the lumpfish.

To identify the size limits at which fish cannot escape from certain net mesh sizes, the industry carries out penetration tests (Harboe and Skulstad, 2013). In these trials, individuals of a range of sizes are tested on the stretched (stiff) square meshes (Fig. 1a) of the cage to see if they are able pass through them. However, the meshes in the netting of a salmon cage are flexible, meaning that they can be deformed to some extent dependent on mesh bar diameter and twine material stiffness. Further, the meshes adopt different shapes depending on the magnitude and direction of the forces to which they are exposed (Herrmann and O'Neill (2006). These forces depend on factors such as weather and sea currents (Huang et al., 2006; Lader et al., 2003, 2008), thus the mesh state in the netting of cages in exposed locations changes frequently, and the meshes often tend to be in semi-slack and slack states (Fig. 1). In addition, many of the operations performed during cage farming involve manipulation of the cage netting, which again results in the meshes in the netting adopting semi-slack or slack states. In a net panel of square meshes, each with two vertical and two horizontal bars (i.e. sides), hanging at sea, the load in the netting is on the vertical bars due to gravity, meaning that the horizontal bars are to a certain extent tensionless and therefore potentially deformable. When the meshes are semi-slack, the fish in the cages could potentially deform the horizontal bars in the meshes while squeezing through them and ultimately escape (Fig. 1b). In situations weather conditions that leads to a sea state with strong sea waves load on the vertical mesh bars will be pulsing, dynamically changing size and direction, potentially resulting in periods where the load on the vertical bars would disappear, making the meshes slack and deformable in all directions (Fig. 1c). Slack and at least some states of semi-slack meshes would lead to a higher risk of escape for lumpfish, simply because the mesh totally (slack) or partially (semi-slack) deforms when adjusting to the shape of lumpfish trying to squeeze through it. Therefore, penetration tests assuming a stable stiff state of the meshes in cage netting likely leads to a serious underestimation of the size of lumpfish that can escape.

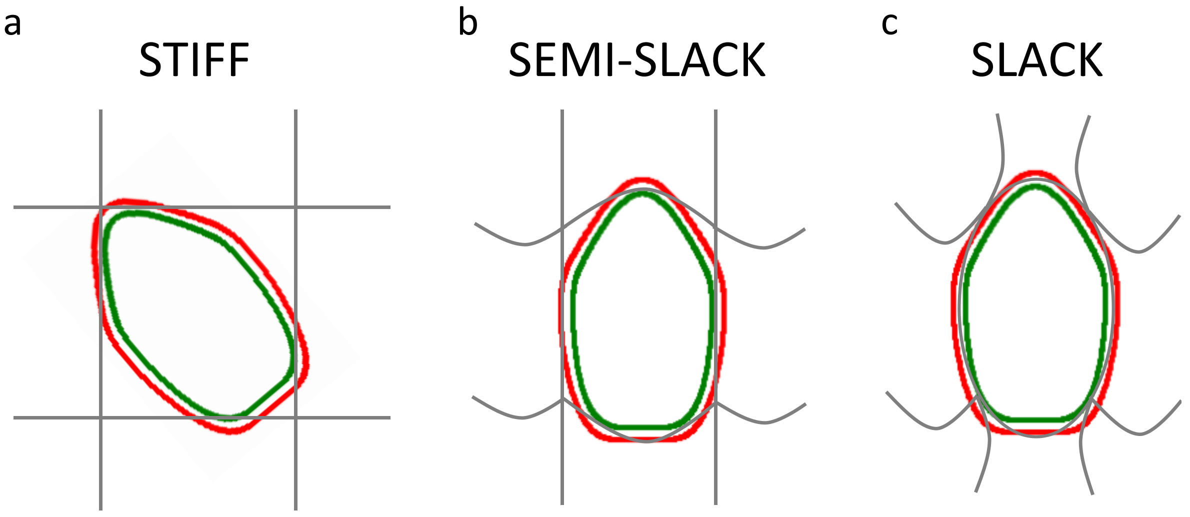

Fig. 1. Mesh penetration of a lumpfish represented by its cross-section (red = uncompressed, green = maximum compression) through a (a) stiff, (b) semi-slack, and (c) slack mesh.

Two factors determine the maximum size at which a lumpfish individual would be able to squeeze through a mesh. The first is the deformability of the meshes in the netting and the second is the deformability or compressibility of the lumpfish tissue. In Figure 1, only a lumpfish with a compressibility level illustrated by the green cross-section (CS) would be able to pass through the square meshes in each of the mesh states (Fig. 1a-c). Thus, different potential netting scenarios in combination with the morphology and cross-sectional compressibility of the species being investigated must be tested to quantify the potential risk of escape for a lumpfish through a specific netting.

2.2. FISHSELECT methodology and data collection

FISHSELECT (Herrmann et al., 2009, 2012) is a framework of methods, tools, and software developed to determine if a fish can penetrate a certain mesh or defined shape. The method has been widely used to predict the size selectivity of fishing gear (the size-dependent probability for escape/retention) (Krag et al., 2011; Sistiaga et al., 2011; Herrmann et al., 2016a,b; Tokaç et al., 2016; Tokaç et al., 2018; Cuende et al., 2020). In the current study, we used this method for the first time to predict the risk of lumpfish escaping through salmon farm cage netting.

Both FISHSELECT software and specific measuring tools are needed to study the size selectivity of a species using this method (Fig. 2). Through computer simulation, the method estimates the risk of escape by comparing the morphological characteristics of a particular fish species and the shape and size of the selection devices of interest. The following subsections briefly describe the different steps needed to use FISHSELECT. A more thorough description of the method can be found in Herrmann et al. (2009, 2012).

2.2.1. FISHSELECT morphometric data collection

In addition to measuring the total length and weight of each individual lumpfish included in the study, its cross-sectional morphology was measured at specific points along its length. To obtain the correct morphometric measures for each fish using FISHSELECT, it is important that the shape of the fish measured is not affected by dehydration, depressurization, rigor mortis, or any other factor that could alter the original shape of the fish. Therefore, the fish for the trials were handpicked in batches of 4–5 fish and killed with an overdose of MS 222 anaesthetic just before use. Our aim with FISHSELECT was to make predictions for mesh penetration probability for the widest possible range of fish sizes. Thus, apart from the condition of the lumpfish selected, the only other selection criterion for fish was that they covered the widest possible size range.

Two cross-sections were selected for their potential to determine fish passage through a mesh: cross-section 1 (CS1), which was located directly behind the operculum, and cross-section 2 (CS2), which was located at the point of the maximum transverse perimeter (i.e., the foremost point of the dorsal fin) (Fig. 2). CS1 represents the point of maximum girth of the bony structure in the head, whereas CS2 represents the point with maximum girth of the fish overall. Thus, these two CSs were expected to be the decisive CSs for mesh penetration. The two cross-sections were measured using a sensing tool called a morphometer. The shapes formed in the morphometer were then scanned to obtain digital images of the contours using a flatbed scanner (Fig. 2).

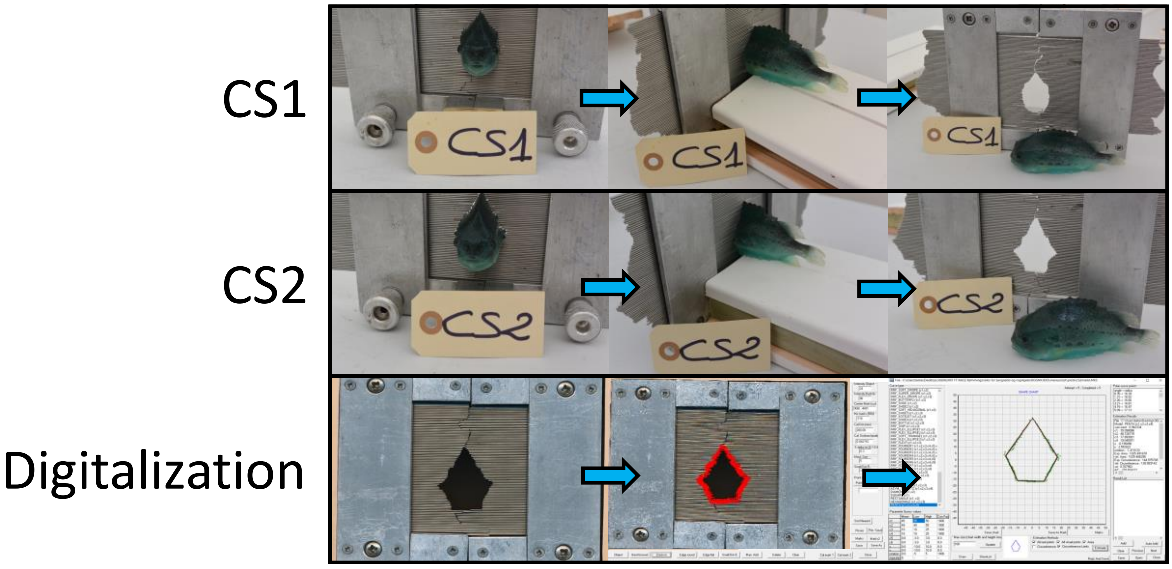

Fig. 2. The first and second rows describe CS1 and CS2, respectively, and the third row shows the process of digitization of the shapes measured by a morphometer.

Models (i.e., numerical representations through parametric shapes) of the digitized cross-sectional images obtained for each lumpfish were developed. For each CS, we initially considered five different shape models: ellipse, flexellipse1, flex drop, super drop, and ship (see Sistiaga et al. (2020) for further information about these five models). The models were selected based on previous experience with other fish species. However, we also had to develop a new model due to the distinctive morphology of lumpfish. This model, which we named penta, is shaped like a pentagon and is defined by four parameters (see the Appendix for further information about the penta model). The Akaike Information Criterion (AIC) (Akaike, 1974) and R^2 values were calculated for each of the six models for both CS1 and CS2 (see Tokaç et al. (2016) for further details about this process). The shape model with the lowest mean AIC value was chosen to describe each of the two cross-sections separately. The mean R^2 value was applied to judge how well the selected models on average described the cross-sectional shapes of lumpfish. The relationship between total length and cross-section shape parameters was modelled for the most suitable shapes found for CS1 and CS2 separately.

2.2.2. Fall-through experiments

After measuring lumpfish morphology, we conducted fall-through experiments to determine whether each lumpfish included in the study could or could not physically pass through an array of stiff mesh shapes perforated in 5 mm nylon-plate templates. Only the force of gravity was used to simulate the attempted penetration of lumpfish through the mesh (Fig. 3). All lumpfish were presented at an optimal orientation for mesh penetration to each of the 478 meshes in the templates. The set of mesh templates used in this experiment consisted of 478 different shapes representing mesh sizes ranging from 20 to 245 mm. The shapes included diamonds (252 meshes), hexagons (98 meshes), and rectangles (128 meshes) and were identical to those described by Tokaç et al. (2016). All lumpfish were presented at an optimal orientation for mesh penetration to each of the 478 meshes in the templates. Compared to using real meshes for the penetration tests, the cut-out meshes in the mesh templates are much more precise and well-defined in shape and size, which is essential for the precision in the results obtained. Penetration (Yes) or retention (No) was recorded for each fish (see Herrmann et al. (2009) for further details about the procedure). The purpose of the fall-through experiments was to estimate the maximum compressibility for a fish trying to squeeze itself through a mesh (see Herrmann et al. (2009) for further details).

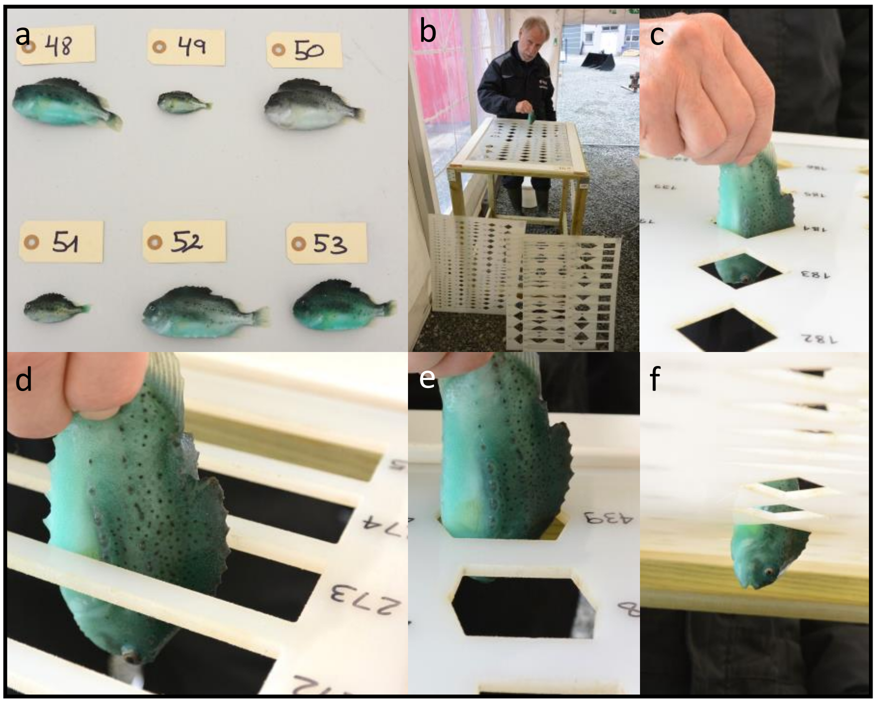

Fig. 3. Photo (a) shows a sample of the different lumpfish sizes used in the fall-through tests, photo (b) shows the different templates employed in the fall-through tests, and photos (c–f) illustrate the fall-through procedure for different lumpfish and meshes.

2.2.3. Simulation of mesh penetration and selection of a penetration model

The shape and compressibility of a lumpfish determines whether it will be able to pass through a mesh. The penetration models implemented in FISHSELECT simulated the compressibility of each fish at each cross-section. Visual and tactile inspection of the deformability of lumpfish revealed that the dorsal and ventral compressibility of this species may differ. Therefore, we applied a model that allows asymmetrical compression for both

CS1 and CS2. Herrmann et al. (2012) previously used this model for redfish (*Sebastes* spp.), and it includes the estimation of three parameters that represent the dorsal, lateral, and ventral compressibility of the fish. The potential compressibility of the fish at an arbitrary angle around the fish cross-section was then modelled by linear interpolation between the potential compressibility (dorsally, laterally, and ventrally) of the fish at each cross-section (see Herrmann et al. (2009) for further details).

To establish an optimal penetration model for lumpfish, each CS1 and CS2 measurement, both individually and in combination, was tested with different compression models using different values for the assumed dorsal, lateral, and ventral compression. The penetration of the modelled CS1 and CS2 shapes of each fish through the 478 different mesh templates used in the fall-through trials was simulated using the FISHSELECT software. The purpose of these simulations was to estimate the compression potential of the cross-sections and to assess which cross-section combinations needed to be considered when estimating the potential for lumpfish to pass through meshes of different sizes and shapes. Models considering one cross-section at a time were created. For CS1, the dorsal, lateral, and ventral compression varied from 0 to 20%, 0 to 30%, and 0 to 30%, respectively, in increments of 5%. This resulted in 245 penetration models for CS1. For CS2, the dorsal, lateral, and ventral compression varied from 0 to 30%, 0 to 20%, and 0 to 40%, respectively, in increments of 5%. This resulted in 315 penetration models for CS2. In addition to the models run for each cross-section, 77,175 models in which CS1 and CS2 were combined were also tested. Each compression model was used to simulate fall-through results for each of the meshes and fish used in the experimental fall-through data collection (Section 2.2.2). Using the FISHSELECT software, the results obtained from all different penetration models were compared with our experimental fall-through results. This evaluation produced a value for the degree of agreement (DA value), which expresses the percentage of the fall-through results for which the simulated results were the same (“yes” or “no”).

2.2.4. Modelling of mesh shapes for square meshes in fish farm cages during lumpfish escape attempts

Before being able to use the generated virtual population of lumpfish and the identified penetration model to predict the risk of lumpfish escape through square meshes in fish farm cages using the FISHSELECT methodology, we needed an appropriate model for the semi-slack mesh state (Fig. 1b) and for the fully slack mesh state (Fig. 1c). In the FISHSELECT simulation, the latter is directly modelled by the condition that a lumpfish can escape if the circumference of its cross-section under maximum compression is less than the inner circumference of the mesh it attempts to pass through. This is because the mesh in this mesh state will be fully distorted while the lumpfish is passing through it. In semi-slack and partly open square meshes (Fig. 1b), the shape the mesh will take when a fish attempts to pass through it was approximated by a hexagonal shape wherein the tensionless horizontal mesh bars are bent upwards and downwards (Fig. 4a–c). This approximation has been applied successfully when modelling fish escape through square mesh codends in trawl and demersal seine fisheries for several species including salmon smolt (Sistiaga et al., 2020), cod (Herrmann et al., 2016a, 2016b), haddock (Krag et al., 2011; Herrmann et al., 2016b), red mullet (Tokaç et al., 2016), and hake (Tokaç et al., 2018).

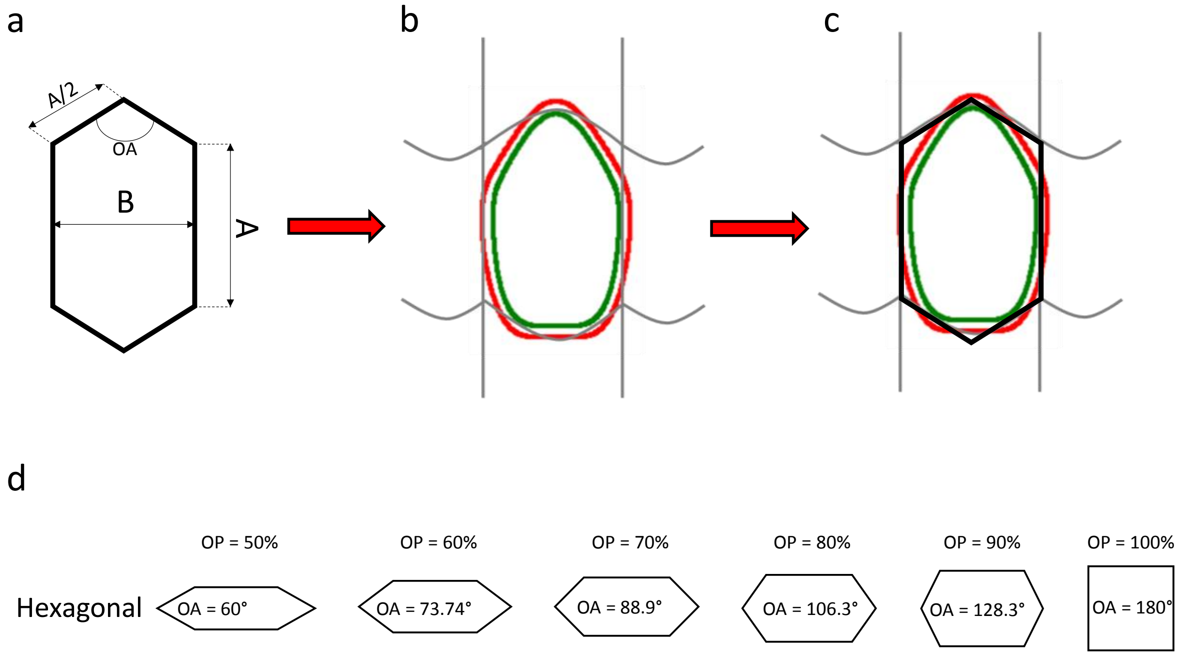

Fig. 4. Hexagonal mesh shape approximation for fish escape through a semi-slack square mesh. (a) Details about hexagonal mesh. (b) Illustration of fish escape through semi-slack square mesh. (c) Approximation of the distorted semi-slack square mesh with a hexagonal shape. (d) Examples of hexagonal shapes approximating distorted semi-slack square meshes with different levels of openness (see Eq. (1)). A = mesh bar length. B = mesh width. OA = opening angle. OP = relative openness.

We applied two related measures to describe the openness of a hexagonal modeled distorted semi-slack square mesh: opening angle (OA) and relative openness (OP). They quantify the circumferential (horizontal) opening of the mesh (B) relative to the vertical opening (A) (Fig. 4a). Figure 4d shows the relationship between OA and OP for hexagonal distorted square meshes, which is calculated as follows:

$$OP = 100 \times \frac{B}{A} = 100 \times sin\left(\frac{OA}{2}\right) \qquad (1)$$

The stiff mesh scenario (Fig. 1a) is a special case for the hexagonal approximation of the semi-slack mesh when OA = 180° corresponding to an OP of 100%.

2.2.5. Quantifying the escape risk

Based on the morphological description of CS1 and CS2 (section 2.2.1.), a virtual population of 2000 lumpfish with uniformly distributed length of up to 25 cm was created to simulate size selection. This upper size limit was selected because predictions for meshes up to 100 mm were desired. For all three mesh scenarios (Fig. 1) the risk of lumpfish escape was simulated for square meshes with a mesh size between 10 and 100 mm in increments of 5 mm. For the semi-slack scenario, approximated by a hexagon, OP values from 50 to 100% were used in increments of 5%. Using the identified lumpfish penetration model, a simulation was created to determine whether each individual in the virtual population could pass through the mesh in each of the mesh scenarios (stiff, semi-slack, slack). Likewise, for the standard application of the FISHSELECT method (Herrmann et al., 2009) we obtained for each mesh a virtual size selection dataset consisting of lumpfish size-dependent counts of individuals (in 1 cm wide length classes) from the virtual population being retained (not able to pass through) and released (being able to pass through), respectively. We then fitted the traditional logit size selection model to the size selection data by maximum likelihood estimation to obtain the values for the model parameters L50 and SR as follows (Wileman et al., 1996):

$$logit(l, L50, SR) = \frac{exp\left(\frac{ln(9)}{SR} \times (l - L50)\right)}{1 + exp\left(\frac{ln(9)}{SR} \times (l - L50)\right)} \qquad (2)$$

where *L50* quantifies the length of lumpfish that have a 50% probability of being retained and the selection range (*SR)* is the difference between *L75* and *L25* (Wileman et al., 1996). Based on the obtained size selection curves, the size of lumpfish having a 99% retention probability (L99; maximum 1% escape risk) was calculated and used as a measure for the minimum safe size that could be kept in the cages. For a logit size selection model, L99 can be calculated as follows (Krag et al., 2014):

$$L99 = L50 + \frac{SR}{ln(9)} \times ln(99) \quad (3)$$

3. Results

3.1. Data collection

The morphology data collection and fall-through experiments were conducted at a lumpfish juvenile rearing plant in Trøndelag (Mid-Norway) in June 2017. During the study period we had continuous access to live fish, which facilitated selection of the individuals necessary to cover the widest possible size span of lumpfish. The FISHSELECT procedure was applied to 100 lumpfish between 49 mm (6 g) and 124 mm (75 g) (Fig. 5).

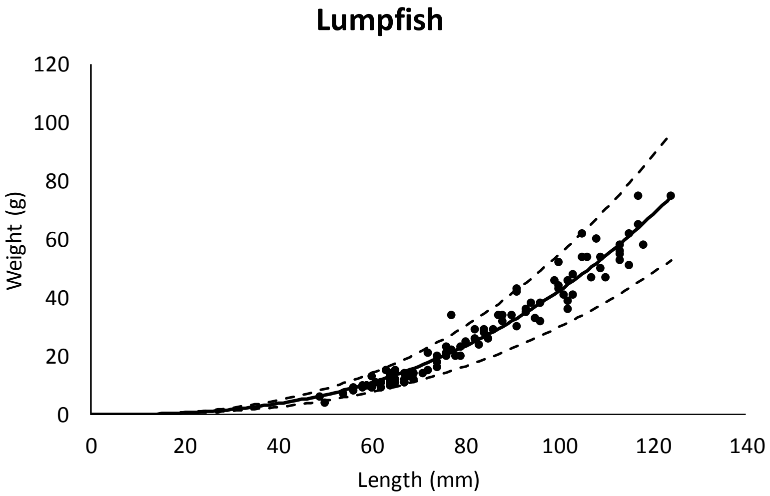

Fig. 5. Weight vs. length relationship for the 100 lumpfish included in the study ($W = a \times L^b$). $a = 2.2249\times10^{-4}$ and $b = 2.64$. $R^2 = 0.9488$. The stippled lines show 95% confidence intervals.

3.2. Cross-section model choice and compressibility of lumpfish

Using computer simulation, the six models considered (section 2.2.1.) were tested on the CS1 and CS2 experimental data to determine which model was best able to describe each CS. The model that resulted in the lowest AIC value was chosen in each case. The model ship, which is a 3-parameter model, was the best representation for CS1, whereas CS2 was best represented by the model penta, which is a 4-parameter model (Table 1). In both cases the R^2 was > 0.94, meaning that the model was able to describe CS1 and CS2 well.

During the fall-through experiments, each lumpfish was tested through 478 meshes of different sizes, meaning that during the experimental period a total of 47,800 fall-through trials were carried out with the 100 fish selected. We used these fall-through results and computer simulation to determine the maximum compression levels for CS1 and CS2. The highest DA between the experimental and simulated fall-through results when considering only the compressibility at CS1 was 97.58%, whereas the highest DA when considering only the compressibility at CS2 was 96.35%. When both CS1 and CS2 were considered, the highest DA achieved was 97.65%. Therefore, this combined compression model was chosen for further analysis and to make mesh penetration predictions for lumpfish in FISHSELECT. The model had a dorsal compression of 5%, lateral compression of 0%, and ventral compression of 0% for CS1 and a dorsal compression of 15%, lateral compression of 10%, and ventral compression of 20% for CS2 (Fig. 6).

Table 1. Comparison of the performance of the six different models tested on the CSs (all models except for penta, which is described in the Appendix, are described in Sistiaga et al., 2020).

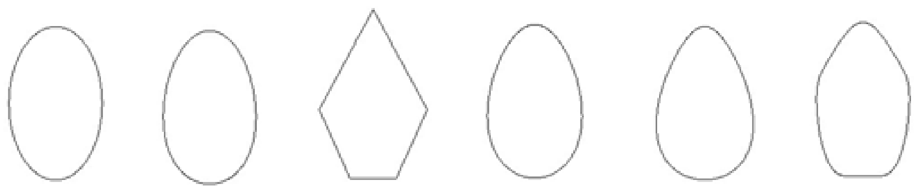

CS models	**Ellipse**		**Flex Ellipse 1**		**Penta**		**Super Drop**		**Flex Drop**		**Ship**	
	CS1	CS2	CS1	CS2	CS1	CS2	CS1	CS2	CS1	CS2	CS1	CS2
AIC	310.00	470.29	271.04	436.61	276.51	**300.28**	268.06	434.01	264.03	403.85	**252.41**	408.67
Nr parameters	2	2	3	3	4	4	3	3	3	3	3	3
R^2	0.9050	0.7653	0.9328	0.8225	0.9301	0.9402	0.9334	0.8247	0.9361	0.8633	0.9419	0.8584

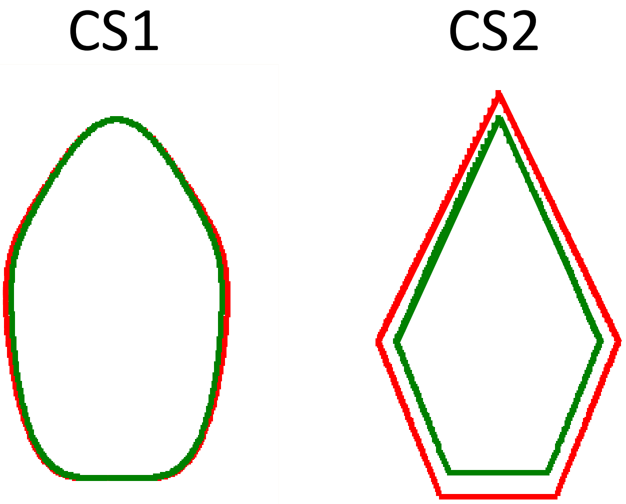

Fig. 6. The combined compression model that provided the highest DA illustrated for one of the 100 lumpfish included in this study. The red contour represents the uncompressed CS, and the green line represents the CS with maximum compression.

3.3. Predictions of mesh penetration and escape risk

Based on a virtual population of 2000 fish, we predicted the escape risk of lumpfish through square meshes of 30 and 50 mm, which are two mesh sizes often used by the salmonid aquaculture industry in Norway. The results showed that if the meshes in the cage netting are completely stiff and perfectly square, lumpfish of up to 46 and 81 mm would be able to escape (< 1% risk) through meshes of 30 and 50 mm, respectively (Fig. 7). In contrast, if the meshes in the cage are completely slack and fully deformable, the escape risk for lumpfish would be higher and fish of up to 61 and 109 mm would be able to escape (< 1% risk) through meshes of 30 and 50 mm, respectively (Fig. 7). If the meshes in the cage are semi-slack, meaning that only the horizontal bars in the meshes are deformable, the escape risk would vary depending on the mesh openness (deformation level of the horizontal bars). For square meshes of 30 mm, the lumpfish size with < 1% escape risk increases to ~52 mm with a mesh openness of ~90% and decreases to 46 mm when the meshes are 100% open (perfectly square meshes). For square meshes of 50 mm, the lumpfish size with < 1% escape risk increases to ~96 mm with a mesh openness of ~90% and decreases to 81 mm when the meshes are 100% open (perfectly square meshes).

The plot in Figure 8 illustrates the minimum size of lumpfish (L99) that can be used for meshes of different sizes and four different states (stiff, semi-slack with 75% mesh openness, semi-slack with 90% mesh openness, and slack meshes). The results clearly show that square meshes in the stiff state allow safe use of the smaller sizes of lumpfish as cleaner fish in the salmon cages without risk of escape into the wild, whereas the meshes need to be substantially reduced in size to maintain the same safety level if the meshes in the cage netting are slack or semi-slack (Fig. 8). For example, to safely retain lumpfish ≥ 150 mm long, the meshes in the cage netting would have to be ≤ 62 mm if the meshes are completely slack at times. However, if the meshes are always stiff, this mesh size could be increased to ~85 mm with the certainty that no fish > 150 mm long would escape. For semi-slack meshes, escape risk with mesh openness > 75% is higher than that of stiff meshes but lower than that of slack meshes. The escape risk for semi-slack meshes is closest to that of slack meshes when the former have an openness of ca. 90 %. This pattern was similar for the whole mesh size range considered (10–100 mm) (Fig. 8).

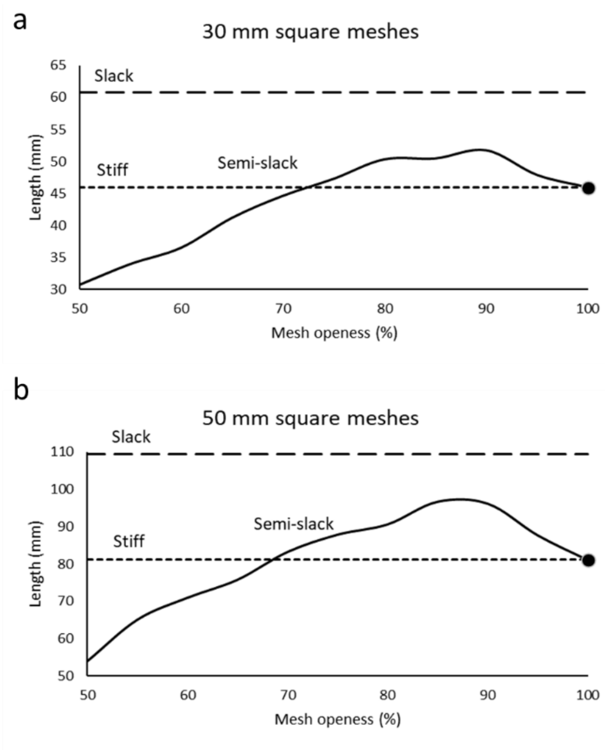

Fig. 7. Sizes of lumpfish with escape risk < 1% (Y axis) as a function of mesh openness (X axis) for semi-slack meshes (solid line). The dashed lines represent the results for slack meshes, and the stippled lines represent the results for stiff meshes. Plot (a) shows the results for 30 mm square meshes and plot (b) shows the results for 50 mm square meshes.

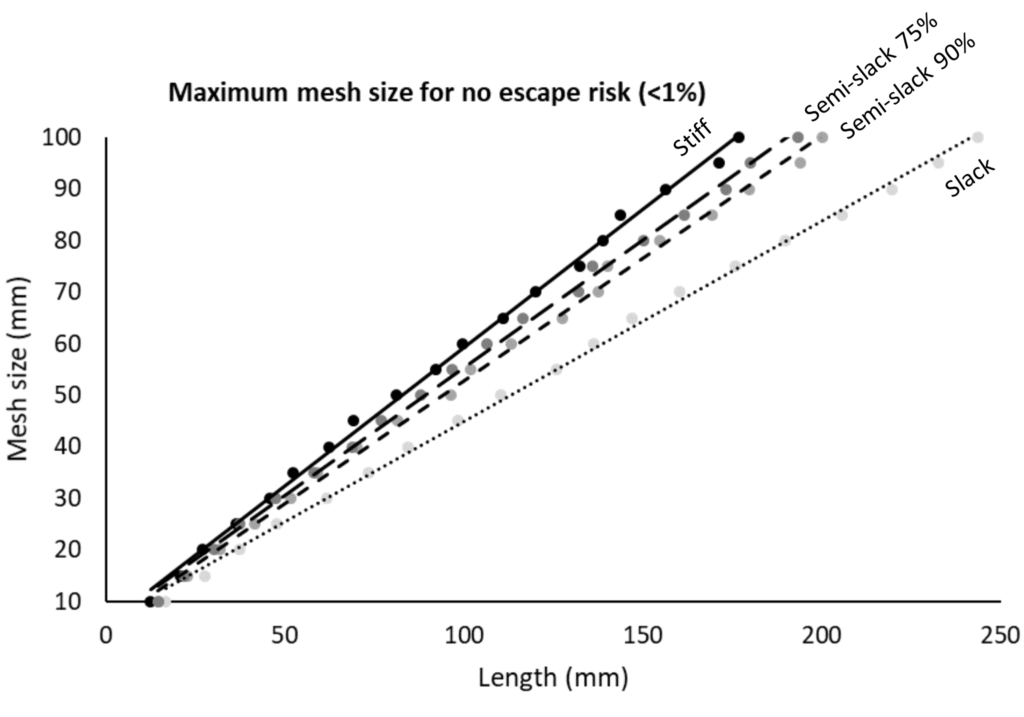

Fig. 8. Maximum square mesh size that guarantees < 1% escape risk as a function of lumpfish size. The lines in the plot show the limits for stiff meshes (full line), slack meshes (dotted line), and semi-slack meshes with 75 and 90% mesh openness (dashed and stippled lines, respectively).

The isolines in the design guide (DG) (Fig. 9) show the smallest sizes of lumpfish that can be safely used (escape risk < 1%) at different mesh size and openness. The DG clearly shows that larger mesh size requires the use of larger lumpfish, independent of mesh openness, to avoid escape risk. Figure 8 also shows that the escape risk for semi-slack meshes with a high degree of openness is larger than for square stiff square meshes (100% openness). For all mesh sizes considered, escape risk increases with mesh openness up to ~90%, and then it decreases to 100% openness, with the same risk as that for square stiff meshes. Thus, if the netting in the cages is changed from 30 mm square meshes to 50 mm square meshes, the minimum size of lumpfish used in the cage should be increased by ~40 mm to maintain an escape risk < 1%, independent of mesh openness.

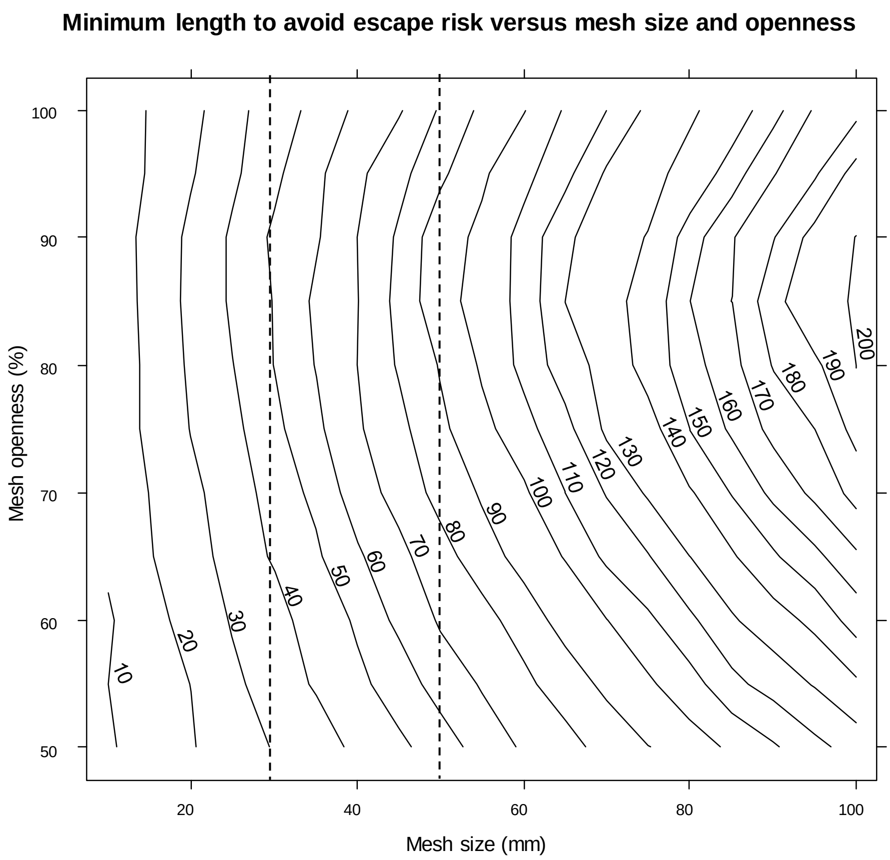

Fig. 9. Isolines showing minimum length of lumpfish (< 1% escape risk) in mm that can be used in farms for square meshes between 20 and 100 mm and mesh openness varying between 50 and 100% in the semi-slack mesh state. The stippled lines show the estimates for the 30 and 50 mm meshes that can be related to Fig. 7.

4. Discussion

Several studies have highlighted the importance of limiting the escape of lumpfish from salmon farming cages (Powell et al., 2018a; Whittaker et al., 2018) to avoid potential problems such as spreading of diseases, outcompeting endemic species, and genetic contamination of surrounding ecosystems (Consuegra et al., 2011; Sepulveda et al., 2013). In the Norwegian aquaculture industry, which is the largest "consumer" of juvenile lumpfish worldwide (Foss et al., 2020), the mesh sizes used in net cages and how they relate to the minimum sizes of lumpfish used are not regulated by law. Farmers use self-developed guidelines based on mesh penetration tests that do not consider potential variations in fish compressibility or different mesh states, which can lead to underestimation of the minimum lumpfish size needed for each mesh size, which in turn may permit escape of reared lumpfish into the wild. Although the extent to which lumpfish escapees occur is not reported in literature, it is acknowledged that this is a problem for the industry that needs to be investigated (e.g. Powell et al., 2018).

In this study, we evaluated the escape risk of lumpfish from salmon farms based on the morphology of the species and the size and state of the meshes used in cage nets. The Norwegian industry typically uses meshes of 30 and 50 mm in the cage nettings (Moe et al., 2007), and the sizes of lumpfish employed can be as low as 6–9 cm in length (Salmar AS, Personal communication). For square meshes of 30 mm, which are often used in the cage nettings, our results show that even the most critical mesh state (slack) would not lead to any significant escape risk (< 1%), as the minimum safe size is estimated to be 6.1 cm. However, for cage nets with 50 mm meshes, the use of 6–9 cm long lumpfish would be of concern.

Even at the least critical mesh state (stiff), lumpfish < 8.1 cm would pose an escape risk. Therefore, to avoid escape risk and the associated risk of biological contamination, lumpfish as small as 6–9 cm should only be used when the mesh size in the net cages is 30 mm. According to our results, use of the 50 mm mesh would only be safe for lumpfish > 11 cm in situations where the meshes likely would go slack at times. For the slack and semi-slack mesh state our predictions assume that lumpfish are able to deform the tensionless mesh bars in the cage netting. In practice, the extent to which lumpfish can do this may depend on the bending stiffness of the mesh bars in the cage netting (Herrmann and O'Neill, 2006). Our results can be seen as “worst-case scenarios”, but they represent the cases that need to be considered in a precautious estimate for escape risk. For the industry, a cautious approach that guarantees a 0-escape scenario through mesh penetration is recommended. This can be achieved by increasing the smallest sizes of lumpfish used a certain percentage above the limits established here, or reducing the mesh sizes further from the limits established, although the latter may imply additional challenges and require trade-offs regarding issues like water flow, fouling, etc.

Compared to other relevant species in the aquaculture industry (e.g. smolt (Sistiaga et al., 2020)), lumpfish are not particularly compressible. Furthermore, they are not good swimmers (Powell et al., 2018b), which suggests limited power to squeeze themselves through meshes. These two characteristics suggest that our escape risk results likely are not underestimated. Our results also illustrate that changes in mesh state (openness) can have dramatic consequences for the penetrability of lumpfish through square meshes (Figs. 7–9), and these changes are not considered in the industry guidelines. The consequence of not considering mesh state is clearly shown in Figure 9. For example, the industry guidelines state that salmon farmers should be able to use lumpfish as small as 67 mm with square meshes of 40 mm (Sigstadstø, 2017). Although this result is in good agreement with our estimations for stiff square meshes, fish > 67 mm long would be able to escape through the 40 mm meshes with mesh openness of 75–95%. Thus, if the meshes in the cage netting are subjected to deformation due to factors such as sea state, sea currents, or maintenance operations in the farm but the minimum size allowed is based on the assumption that escape only occurs through stiff square meshes, there could be substantial risk of lumpfish escape.

Because farmers prefer to use small lumpfish, it is likely that the lumpfish added to the cages are as close to the established lower size limit as possible, which substantially increases the risk of escape. The preference for small lumpfish is driven by their delousing efficiency, which has been reported to decrease with increasing size (Imsland et al., 2014a,b,c). Additional advantages include shorter rearing time (costs) and the possibility for coexistence with wrasses, which can be harassed by larger lumpfish (Imsland et al., 2016). However, smaller inexperienced lumpfish show more avoidance behavior towards salmon than larger individuals (Staven et al., 2019). This initial behavior of avoiding contact with salmon can lead small lumpfish to attempt escape from the cages. If this potential fleeing behavior is added to the inherent increase in escape risk due to their smaller size, the sustainability of using the smallest sizes of lumpfish is questionable.

The escape of lumpfish from aquaculture cages has multiple implications. For example, escape increases the cost for the industry, as lumpfish escapees need to be replaced to maintain delousing capacity. However, the most important socio-economic implication of losing reared lumpfish to the wild is related to the potential environmental threat that escapees pose. According to Jónsdóttir et al. (2018), the genetic diversity of wild lumpfish along the Norwegian coast is so low that if individuals translocated within the country escape from aquaculture stations, they would probably have little to no impact on the genetic composition of the local fish populations. However, this low genetic diversity makes these local populations vulnerable to genetic introgression from other populations (Whittaker et al., 2018). Considering the exponential increase in demand for lumpfish in the last decade, translocation of individuals from non-Norwegian populations likely will occur in the near future. This scenario poses an additional threat to wild lumpfish populations that are already overexploited due to capture of mature wild individuals for use as broodstock and at risk of diseases spread by escapees from salmon farms (Powell et al., 2018a).

Salmon farmers need to consider multiple factors when choosing lumpfish sizes to use in their cages, including the interaction with other species in the cages, delousing efficiency, and rearing cost. Our results highlight the importance of also considering potential changes in mesh state (i.e., how exposed the netting is to sea state and currents) and the morphological properties of lumpfish when determining the minimum sizes of fish to be used. Finally, the results presented here can be used to develop new guidelines for scientists and the industry that will contribute to reducing the escape risk of lumpfish from salmonid farms and the consequent potential environmental issues posed by escapees.

Acknowledgements

We would like to thank SINTEF Ocean (RACE program Project number 302002497) and the Institute of Marine research in Norway for financing the field trials and the posterior data analysis and reporting of results. We are grateful to Reviewer Dr. Steve I. Lonhart, whose valuable comments and suggestions helped us significantly improving the final version of this manuscript.

References

Aaen, S.M., Helgesen, K.O., Bakke, M.J., Kaur, K., Horsberg, T.E., 2015. Drug resistance in sea lice: a threat to salmonid aquaculture. Trends Parasitol. 31, 72–81.

Abolofia, J., Asche, F., Wilen, J.E., 2017.The cost of lice: quantifying the impacts of parasiticsea lice on farmed salmon. Mar. Resour. Econ. 32, 329–349.

Bjordal Å (1991) Wrasse as cleaner- fish for farmed salmon. Progress in Underwater Science 16: 17– 28.

Brooker, A.J., Papadopoulou, A., Gutierrez, C., Rey, S., Davie, A., Migaud, H., 2018. Sustainable production and use of cleaner fish for the biological control of sea lice: recent advances and current challenges. Vet. Rec.183(12), 383.

Consuegra, S., Phillips, N., Gajardo, G., de Leaniz C.G., 2011. Winning the invasion roulette: escapes from fish farms increase admixture and facilitate establishment of non-native rainbow trout. Evolutionary Applications 4, 660–671.

Cuende, E., Arregi, L., Herrmann, B., Sistiaga, M., Aboitiz, X., 2020. Prediction of square mesh panel and codend size selectivity of blue whiting based on fish morphology. ICES Journal of Marine Science, published online 24 September 2020. https://doi.org/10.1093/icesjms/fsaa156.

Foss, A., Imsland, A.K.D., Roth, B., Nytrø, A.V., 2020. Catch me if you can: How to recapture lumpfish using light as an attractant. Aquacultural engineering 90, 102074.

Geitung, L., Wright, D.W., Oppedal, F., Stien, L.H., Vågset, T., Madaro, A., 2020. Cleaner fish growth, welfare and survival in Atlantic salmon sea cages during an autumn-winter production. Aquaculture 528, 735623.

González, E. B. & de Boer, F. The development of the Norwegian wrasse fishery and the use of wrasses as cleaner fish in the salmon aquaculture industry. Fish. Sci. 83, 661–670 (2017).

Gonzalez, E. B., and de Boer, F. 2017. The development of the Norwegian wrasse fishery and the use of wrasses as cleaner fish in the salmon aquaculture industry. Fisheries Science, 83: 661–670.

Harboe, T., Skulstad, O.F., 2013. Undersøkelse Av Maskeåpning Og Smoltstørrelse. Institute of Marine Research, Nr. 22–2013. 22pp. In Norwegian). Institute of Marine Research, Postbox 1870 Nordnes, 5817 Bergen, Norway.

Herrmann, B., O'Neill, F.G., 2006. Theoretical study of the influence of twine thickness on haddock selectivity in diamond mesh cod-ends. Fisheries Research 80: 221-229.

Herrmann, B., Krag, L., Frandsen, R., Madsen, N., Lundgren, B., Stæhr, K.J., 2009. Prediction of selectivity from morphological conditions: Methodology and case study on cod (*Gadus morhua*). Fisheries Research 97: 59-71.

Herrmann, B., Sistiaga, M., Nielsen, K.N., Larsen, R.B., 2012. Understanding the size selectivity of redfish (*Sebastes spp.*) in North Atlantic trawl codends. Journal of Northwest Atlantic Fishery Science (ISSN: 1813-1859), vol: 44, pages: 1-13.

Herrmann, B., Larsen, R.B., Sistiaga, M., Madsen, N.H.A., Aarsæther, K.G., Grimaldo, E., Ingolfsson, O.A., 2016a. Predicting size selection of cod (*Gadus morhua*) in square mesh codends for demersal seining: a simulation-based approach. Fish. Res. 184, 36–46.

Herrmann, B., Krag, L.A., Feekings, J., Noack, T., 2016b. Understanding and predicting size selection in diamond mesh codends for Danish seining: a study based on sea trials and computer simulations. Marine and Coastal Fisheries 8: 277-291.

Huang, C.-C., Tang, H.-J., Liu, J.-Y., 2006. Dynamical analysis of cage structures for marine aquaculture: numerical simulation and model testing. J. Aquac. Eng. Fish. Res. 35, 258–270.

Imsland, A.K., Reynolds, P., Eliassen, G., Hangstad, T.A., Nytrø, A.V., Foss, A., Vikingstad, E., Elvegård, T.A., 2014a. Notes on behaviour of lumpfish in sea pens with and without Atlantic salmon. J. Ethol. 32, 117–122.

Imsland, A.K., Reynolds, P., Eliassen, G., Hangstad, T.A., Foss, A., Vikingstad, E., Elvegård, T.A., 2014b. The use of lumpfish (*Cyclopterus lumpus* L.) to control sea lice (Lepeophtheirus salmonis Krøyer) infestations in intensively farmed Atlantic salmon (Salmo salar L.). Aquaculture 425-426, 18–23.

Imsland, A.K., Reynolds, P., Eliassen, G., Hangstad, T.A., Nytrø, A.V., Foss, A., Vikingstad, E., Elvegård, T.A., 2014c. Assessment of growth and sea lice infection levels in Atlantic salmon stocked in small-scale cages with lumpfish. Aquaculture 433, 137–142.

Imsland, A.K., Reynolds, P., Nytrø, A.V., Eliassen, G., Hangstad, T.A., Jónsdóttir, Ó.D.B., Emaus, P.A., Elvegård, T.A., Lemmens, S.C.A., Rydland, R., Jonassen, T.M., 2016. Effects of lumpfish size on foraging behaviour and co-existence with sea lice infected Atlantic salmon in sea cages. Aquaculture 465, 19–27.

Imsland, A.K.D., Reynolds, P., Lorentzen, M., Eilertsen, R.A., Micallef, G., Tvenning, R., 2020. Improving survival and health of lumpfish (*Cyclopterus lumpus L.*) by the use of feed blocks and operational welfare indicators (OWIs) in commercial Atlantic salmon cages. Aquaculture 527, 735476.

Johannesson, J., 2006. Lumpfish Caviar: From Vessel to Consumer. Food & Agriculture Organization Fisheries Technical paper, No. 485. FAO, Rome, 60p.

Jonassen T, Remen M, Lekva A, Steinarsson A, Árnason T. 2018a. Transport of lumpfish and wrasse. In: Treasurer JW, ed. Cleaner fish biology and aquaculture applications. Sheffield: 5M Publishing Ltd. 319-335.

Jónsdóttir, Ó. D. B., Schregel, J., Hagen, S., Tobiassen, C., Aarnes, S. G. and Imsland, A. K. D., 2018. Population structure of lumpfish along the Norwegian coast: aquaculture implications. Aquac. Int. 26, 49-60.

Jónsdóttir KE, Hvas M, Alfredsen JA, Fore M, Alver MO, Bjelland HV, Oppedal, F., 2019. Fish welfare based classification methodof ocean current speeds at aquaculture sites. Aquaculture Environment Interactions 11, 249– 261.

Kennedy J, Durif CMF, Florin AB, Frechet A, Gauthier J, Hussy K et al. 2019 A brief history of lumpfishing, assessment, and management across the North Atlantic. Ices Journal of Marine Science 76: 181– 191.

Klakegg, Ø., Myhren, S., Juell, R.A., Aase, M., Salonius, K., Sørum, H., 2020. Improved health and better survival of farmed lumpfish (*Cyclopterus lumpus*) after a probiotic bath with two probiotic strains of *Aliivibrio*. Aquaculture 518, 734810.

Lader, P., Dempster, T., Fredheim, A., Jensen, Ø. 2008. Current induced net deformations in full-scale sea-cages for Atlantic salmon (*Salmo salar*). J. Aquac. Eng. Fish. Res. 38, 52–65.

Lorance P, Cook R, Herrera J, de Sola L, Florin A, Papaconstantinou C. 2015. Cyclopterus lumpus. The IUCN Red List of Threatened Species 2015 e.T18237406A45078284. http://www.iucnredlist.org/details/18237406/1

Moe, H., Olsen, A., Hopperstad, O.S., Jensen, Ø., Fredheim, A., 2007. Tensile properties for netting materials used in aquaculture net cages. J. Aquac. Eng. Fish. Res. 37, 252–265.

Overton, K., Dempster, T., Oppedal, F., Kristiansen, T.S., Gismervik, K., Stien, L.H., 2018. Salmon lice treatments and salmon mortality in Norwegian aquaculture: a review. Reviews in Aquaculture: 1-20.

Powell, A., Treasurer, J.W., Pooley, C.L., Keay, A.J., Lloyd, R., Imsland, A.K., Garcia de Leaniz, C., 2018a. Cleaner fish for sea-lice control in salmon farming: challenges and opportunities using lumpfish. Rev. Aquac. 10, 683–702.

Powell, A., Pooley, C., Scolamacchia, M., Garcia de Leaniz, C., 2018b. Review of lumpfish biology. In: Cleaner fish biology and aquaculture applications. Treasurer J. W. (ed.). 5M Publications. Sheffield. pp. 98-121.

Sayer, M.D.J., Reader, J.P., 1996. Exposure of goldsinny, rock cook and corkwing wrasse to low temperature and low salinity: Survival, blood physiology and seasonal variation. J. Fish Biol. 49, 41–63.

Sepulveda, M., Arismendi, I., Soto, D., Jara, F., Farias, F., 2013. Escaped farmed salmon and trout in Chile: Incidence, impacts, and the need for an ecosystem view. Aquaculture Environment Interactions, 4, 273–283.

Sigstadstø, 2017. Veileder for bruk og hold av rognkjeks. www.lusedata.no (*In Norwegian*).

Sistiaga, M., Herrmann, B., Forås, E., Frank, k., Sunde, L.M., 2020. Prediction of size-dependent risk of salmon smolt (*Salmo salar*) escape through fish farm nets. Aquacultural Engineering 89, 102061.

Staven, F. R., Nordeide, J. T., Imsland, A. K., Andersen, P., Iversen, N. S., Kristensen, T., 2019. Is habituation measurable in Lumpfish *Cyclopterus lumpus* when used as cleaner fish in Atlantic salmon *Salmo salar* aquaculture? Frontiers in Veterinary Science, 6, 227.

Tokaç, A., Herrmann, B., Gökçe, G., Krag, L.A., Ünlüler, A., Nezhad, D.S., Lök, A., Kaykaç, H., Aydın, C., Ulaş, A., 2016. Understanding the size selectivity of red mullet (Mullus barbatus) in Mediterranean trawl codends: A study based on fish morphology. Fisheries Research 174: 81-93.

Tokaç, A., Herrmann, B., Gökçe, G., Krag, L.A., Nezhad, D.S., 2018. The influence of mesh size and shape on the size selection of European hake (Merluccius merluccius) in demersal trawl codends: An investigation based on fish morphology and simulation of mesh geometry. Scientia Marina, vol 82, 147-157.

Torrissen, O., Jones, S., Asche, F., Guttormsen, A., Skilbrei, O.T., Nilsen, F., Horsberg, T.E., Jackson, D., 2013. Salmon lice—impact on wild salmonids and salmon aquaculture. J. Fish Dis. 36, 171–194.

Treasurer, J.W., 2018. An introduction to sea lice and the rise of cleaner fish. Cleaner Fish Biology and Aquaculture Applications. In: Treasurer JW, ed. Cleaner fish biology and aquaculture applications. Sheffield: 5M Publishing Ltd. 3-24.

Whittaker BA, Consuegra S, Garcia de Leaniz C. 2018 Genetic and phenotypic differentiation of lumpfish (*Cyclopterus lumpus*) across the North Atlantic: implications for conservation and aquaculture. PeerJ 6, e5974.

Wootten, R., Smith, J.W., Needham, E.A., 1982. Aspects of the biology of the parasitic copepods *lepeophtheirus salmonis* and *caligus elongatus* on farmed salmonids, and their treatment. Proc. Royal Soc. Biol. Sci. 81, 185–197.

Appendix

This appendix contains a description of the penta model considered to describe the cross-section shape of lumpfish. The penta model is defined by the two widths c_1 and c_3 together with the two heights c_2 and c_4 (Fig. A1).

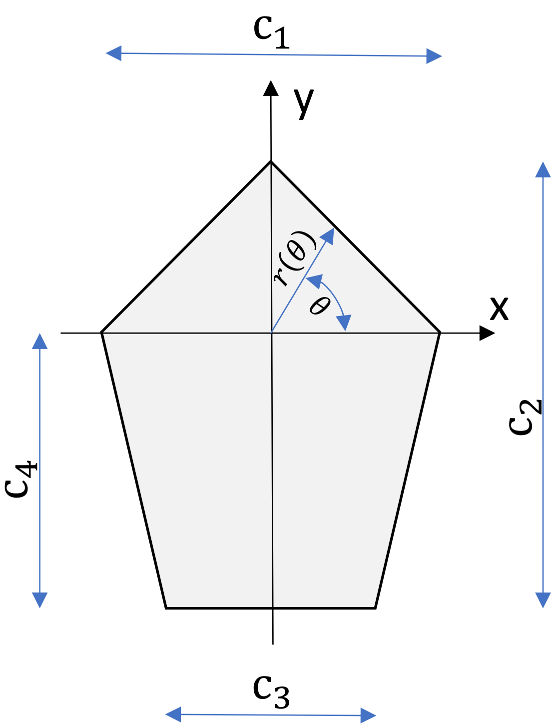

FIG A1: Description of the penta shape model and its parameters.

The description in polar coordinates (θ, r) of the penta shape becomes:

$$r(\theta) = \begin{cases} \dfrac{c_2 - c_4}{sin(\theta)} + 2 \times \dfrac{c_2 - c_4}{c_1} \times cos(\theta);\ \forall\, \theta \in \left[0.0; \dfrac{\pi}{2}\right] \\ \dfrac{c_2 - c_4}{sin(\theta)} - 2 \times \dfrac{c_2 - c_4}{c_1} \times cos(\theta);\ \forall\, \theta \in \left]\dfrac{\pi}{2}; \pi\right] \\ -\dfrac{c_1 \times c_4}{(c_1 - c_3) \times sin(\theta)} + 2.0 \times \dfrac{c_4}{c_1 - c_3} \times cos(\theta);\ \forall\, \theta \in]\pi; \varphi_1] \\ -\dfrac{c_4}{sin(\theta)};\ \forall\, \theta \in]\varphi_1; \varphi_2] \\ -\dfrac{c_1 \times c_4}{(c_1 - c_3) \times sin(\theta)} - 2.0 \times \dfrac{c_4}{c_1 - c_3} \times cos(\theta);\ \forall\, \theta \in]\varphi_2; 2\pi] \end{cases}$$

where

$$\varphi_1 = \tan^{-1}\left(\frac{-c_4}{-0.5 \times c_3}\right)$$
$$\varphi_2 = \tan^{-1}\left(\frac{-c_4}{0.5 \times c_3}\right)$$

Declaration of interests

☒ The authors declare that they have no known competing financial interests or personal relationships that could have appeared to influence the work reported in this paper.

☐The authors declare the following financial interests/personal relationships which may be considered as potential competing interests:

Bent Herrmann
Manu Sistiaga
Terje Jørgensen

CRediT author statement

Bent Herrmann: Conceptualization, Methodology, Software, Validation, Formal Analysis, Investigation, Data curation, Writing – Original Draft –Review & Editing, Visualization.

Manu Sistiaga: Conceptualization, Methodology, Validation, Formal Analysis, Investigation, Data curation, Writing – Original Draft –Review & Editing, Visualization, Project administration, Funding acquisition.

Terje Jørgensen: Writing – Original Draft, Project administration, Funding acquisition.